Composites Science and Technology **49** (1993) 61–69

A UNIT-CELL MODEL OF TEXTILE COMPOSITE BEAMS FOR PREDICTING STIFFNESS PROPERTIES

Bhavani V. Sankar & Ramesh V. Marrey

Department of Aerospace Engineering, Mechanics & Engineering Science, University of Florida, Gainesville, Florida 32611-2031, USA

(Received 25 March 1992; revised version received 9 September 1992; accepted 2 November 1992)

Abstract

Flexural stiffness properties of a textile composite beam are obtained from a finite-element model of the unit cell. Three linearly independent deformations, namely, pure extension, pure bending and pure shear, are applied to the unit cell. The top and bottom surfaces of the beam are assumed to be traction free. Periodic boundary conditions on the lateral boundaries of the unit cell are enforced by multi-point constraint elements. From the forces acting on the unit cell, the flexural stiffness coefficients of the composite beam are obtained. The difficulties in determining the transverse shear stiffness are discussed, and a modified approach is presented. The methods are first verified by applying them to isotropic and bimaterial beams for which the results are known, and then illustrated for a simple plain-weave textile composite.

Keywords: textile composites, woven composites, micromechanics, unit cell analysis, homogenization, finite elements

1 INTRODUCTION

Recent advances in textile manufacturing processes and resin transfer molding techniques have led to the development of what are known as textile structural composites. Advanced fibers such as graphite and glass can be woven or braided into structural preforms. The dry preforms can then be impregnated with appropriate matrix materials, e.g. thermosetting and thermoplastic resins, to fabricate composite structures. Significant progress has been made in the manufacturing processes of these novel materials. There is great potential for the extension of this technology to metal- and ceramic-matrix composites. With the development of textile structural composites there is a need for analytical/numerical models for predicting the mechanical behavior of these materials from the fiber, matrix and fiber/matrix interface properties, and the fiber architecture. Ishikawa and Chou,[1–5] Yang and Chou,[6] and Ma *et al.*,[7] have proposed several models for estimating the thermo-elastic and mechanical properties of woven and braided composites. In Refs 1–5, the unit cell of the woven composite was modeled by using classical lamination theories to predict the stiffness coefficients ([A], [B], [D]) of the textile composite. References 6 and 7 are concerned with elastic constants such as E_x, E_y, etc. of the textile composite. Foye,[8] Whitcomb,[9] Yoshino and Ohtsuka,[10] and Dasgupta *et al.*[11] analyzed the unit cell of textile composites by using three-dimensional finite elements to predict the overall macroscopic behavior of the composites. Their models can be used to predict both stiffness and strength properties.

Numerical modeling of the unit cell seems to be popular because of its ability to capture the effects of complicated fiber architectures. These models are based on the assumption that a composite structural element can be formed by assembling the unit cells in all three dimensions. Such an assumption is true in the case of thick composites, but in many applications one or two layers of fabric are used, e.g. skin of a semi-monocoque structure, frames, ribs, stiffeners, etc. In that case there will be one or two unit cells in the thickness direction, and hence the free surface effects will be significant. Furthermore, the in-plane stresses and displacements will vary through the thickness, violating the assumption of homogeneous deformation in all the unit cells. The elastic constants estimated using the three-dimensional analysis of the unit cell may not be applicable to thin composites. This can be illustrated by a simple example as follows. Consider a composite medium consisting of alternating layers of two isotropic materials with Young's moduli E_1 and E_2, and thickness h_1 and h_2. Any available homogenization scheme will predict that this material can be represented as an orthotropic material with an equivalent in-plane Young's modulus $E_{eq} = (E_1 h_1 + E_2 h_2)/(h_1 + h_2)$, which is same as the

Composites Science and Technology 0266-3538/93/$06.00

simple rule of mixtures. Now, consider a bimaterial beam consisting of the same two layers. The flexural modulus D_{11} of the beam, in general, is not equal to $E_{eq}(h_1+h_2)^3/12$. Further the bimaterial beam will exhibit extension/bending coupling, which cannot be predicted if the beam were considered orthotropic. This illustrates the difference between a structure having a large number of unit cells and that with fewer unit cells in the thickness direction. Then it will be useful to predict the in-plane and flexural properties of the composite directly, instead of the three-dimensional elastic constants. The present paper demonstrates such an idea for a woven fabric composite.

2 UNIT-CELL ANALYSIS FOR THREE-DIMENSIONAL ELASTIC CONSTANTS

In this section a procedure for determining the three-dimensional elastic constants from the unit cell analysis is described. Later, this method is used to determine the shear modulus G_{xz}, and the results compared with the transverse shear stiffness of a thin textile beam. The unit-cell analysis assumes that the material is subjected to a uniform state of strain in a macroscopic sense. The average stresses required to create such a state of strain is computed from the finite element model of the unit cell. In the microscale all unit cells have identical displacement, strain and stress fields. Continuity of stresses across a unit cell then requires that tractions be equal and opposite at corresponding points on opposite faces of the unit cell (periodic boundary conditions). Since the displacement gradients are constant for a homogeneous deformation, the displacements at corresponding points on opposite faces of the unit cell differ only by a constant.

Consider a rectangular parallelpiped with sides parallel to the coordinate axes x_1, x_2 and x_3 as the unit cell. Let the length of the unit cell in the x_i direction be L_i. A macroscopically homogeneous deformation can be represented as

$$u_i = H_{ij}x_j, \quad i,j = 1, 2, 3 \tag{1}$$

where H_{ij} are the displacement gradients. Then the periodic displacement boundary conditions to be imposed on the faces $x_i = 0$ and $x_i = L_i$ are

$$u_i(L_1, x_2, x_3) - u_i(0, x_2, x_3) = H_{i1}L_1 \tag{2}$$

$$u_i(x_1, L_2, x_3) - u_i(x_1, 0, x_3) = H_{i2}L_2 \tag{3}$$

$$u_i(x_1, x_2, L_3) - u_i(x_1, x_2, 0) = H_{i3}L_3 \tag{4}$$

The traction boundary conditions on the faces $x_i = 0$ and $x_i = L_i$ are

$$T_i(L_1, x_2, x_3) = -T_i(0, x_2, x_3) \tag{5}$$

$$T_i(x_1, L_2, x_3) = -T_i(x_1, 0, x_3) \tag{6}$$

$$T_i(x_1, x_2, L_3) = -T_i(x_1, x_2, 0) \tag{7}$$

The above boundary conditions can be imposed by using multi-point constraint elements in the finite-element model. The average macroscopic stresses corresponding to the homogeneous deformations are obtained by averaging the tractions on each face of the unit cell. For example,

$$\sigma_{1j} = \left(\frac{1}{L_2L_3}\right)\sum_n F_j^{(n)} \tag{8}$$

where $F_j^{(n)}$ is the nodal force in the j direction at the nth node, and $\sum_n$ denotes summation over all nodes on the face $x_1 = L_1$. The other stress components can be computed in a similar fashion. The macroscopic tensorial strains are given as $\epsilon_{ij} = (\frac{1}{2})(H_{ij} + H_{ji})$.

In implementing this procedure H_{ij} is chosen such that only one component of strain is non-zero, and the corresponding stresses are computed by the method described above. Substituting the values of the strain and the stresses in the stress/strain relationships, the stiffness coefficients in a column corresponding to the non-zero strain can be evaluated. This procedure is repeated for other strain components to obtain all the stiffness coefficients, from which the elastic constants of the homogeneous material can be determined. In applying this method care should be taken in discretizing the unit cell such that opposite faces of the unit cell have identical nodes.

As mentioned earlier this approach assumes that the unit cells repeat themselves in all three directions. This may not be true in the case of thin textile structural composites where there may be a finite number of unit cells in the thickness direction, and free surface effects will then be predominant. The displacement gradients through the thickness may be significant and hence the assumption of homogeneous deformation will be violated. Then the homogeneous elastic constants will not be useful in predicting the beam/plate behavior. In such a case the composite can be idealized as a homogeneous beam/plate, and the beam/plate stiffness coefficients can be directly computed using a similar method. The extension of the unit cell approach to compute stiffness properties of a textile composite beam is explained in the next section.

3 FLEXURAL STIFFNESS COEFFICIENTS

In this section a procedure for finding the equivalent flexural stiffness properties of a textile structural composite beam is described. The textile composite beam is assumed to be in the xz plane with unit cells repeating in the x direction. A state of plane strain parallel to the xz plane is assumed. The idea behind using a beam model to illustrate the proposed method and its scope are similar to the one-dimensional fabric

strip models presented by Ishikawa and Chou[5] and Yoshino and Ohtsuka.[10] On the macroscale it is assumed that the beam is homogeneous and its behavior can be characterized by the following beam constitutive relations:

$$\begin{bmatrix} K_{11} & K_{12} & K_{13} \\ K_{12} & K_{22} & K_{23} \\ K_{13} & K_{23} & K_{33} \end{bmatrix} \begin{Bmatrix} \epsilon_0 \\ \kappa \\ \gamma_0 \end{Bmatrix} = \begin{Bmatrix} P \\ M \\ V \end{Bmatrix} \tag{9}$$

where $[K]$ is the symmetric matrix of beam stiffness coefficients; ϵ_0, κ and γ_0 are the mid-plane axial strain, curvature and shear strain, respectively; P, M and V are the axial force, bending moment and shear force resultants respectively in the homogeneous beam. The mid-plane deformations are related to the mid-plane axial displacement u_0, transverse displacement w, and rotation ψ as

$$\epsilon_0 = \frac{\partial u_0}{\partial x}, \quad \kappa = \frac{\partial \psi}{\partial x}, \quad \gamma_0 = \psi + \frac{\partial w}{\partial x} \tag{10}$$

Actually K_{11}, K_{12}, K_{22} and K_{33} are similar to the laminate stiffness coefficients A_{11}, B_{11}, D_{11} and $\kappa_1^2 A_{55}$ respectively. There is no equivalence for K_{13} and K_{23} in the laminate theory, because the layers are assumed be orthotropic (or transversely isotropic), and they are rotated about the z axis only. However, such a coupling between in-plane deformations and transverse shear deformation may exist in textile composites as the fibers are inclined to the xy plane unlike in the laminates. Further the present approach cannot be used to predict stiffness properties involving the y direction, such as A_{12}, A_{22}, D_{12}, D_{22} etc. However, their effects are not being neglected because a state of plane strain parallel to the xz plane has been assumed, and hence ϵ_{yy}, γ_{xy} etc. are all taken as equal to zero. The beam constitutive relationships in eqn (9) can also be expressed in terms of compliance coefficients:

$$\begin{bmatrix} S_{11} & S_{12} & S_{13} \\ S_{12} & S_{22} & S_{23} \\ S_{13} & S_{23} & S_{33} \end{bmatrix} \begin{Bmatrix} P \\ M \\ V \end{Bmatrix} = \begin{Bmatrix} \epsilon_0 \\ \kappa \\ \gamma_0 \end{Bmatrix} \tag{11}$$

3.1 Steady-state loading conditions

As discussed earlier the unit-cell analysis assumes that all the unit cells are subjected to identical displacement, stress and strain fields. This is true only for the cases of constant axial force and constant bending moment in the beam (Figs 1(a) and 1(b)). A constant shear force state cannot be created because the shear force will always give rise to building up of bending moment as $V = -(dM/dx)$. A state where the unit cells are subjected to identical deformation under a shear force can be created by adding a couple periodically (Fig. 1(c)) or by having shear tractions on the top and bottom surfaces to cancel the bending moment continuously (Fig. 1(d)). In both cases traction-free conditions are violated on the top and bottom surfaces of the beam. As will be seen later, this situation creates difficulties in estimating the shear stiffness of the beam accurately.

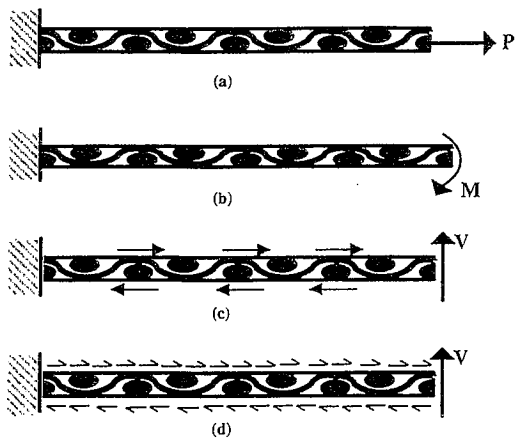

Fig. 1. Steady-state loading of a beam.

3.2 Unit-cell boundary conditions

The equivalent properties are obtained by modeling the unit cell with two-dimensional plane strain finite elements in the xz plane, and applying three linearly independent deformations to the unit cell separately. It means that the differences in displacements between corresponding points on the left and right faces of the unit cell will be equal to that in a homogeneous beam subjected to the same type of deformation. The three macroscopic deformations applied to the unit cell are (i) a unit axial strain: (ii) a unit curvature accompanied by a transverse deflection such that the shear strain γ_{xz} vanishes; and (iii) a unit transverse shear strain. The left end, $x = 0$, of the unit cell is subjected to minimum support constraints to prevent rigid body translation and rotation. The top and bottom surfaces of the beam are considered as free

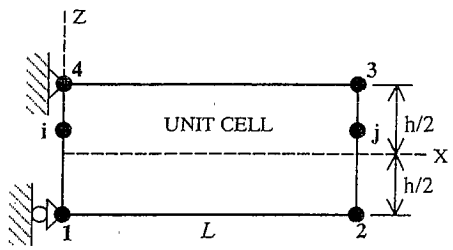

Type of deformation	$u(L,z)-u(0,z)$	$w(L,z)-w(0,z)$
unit axial strain	L	0
unit curvature	Lz	$-L^2/2$
unit shear strain	0	L

Fig. 2. Definition of unit deformations applied to the unit cell.

surfaces. The edges $x=0$ and $x=L$ have identical nodes in the finite-element model and the displacements along these edges are constrained by using special constraint elements. The constraints applied for each case of deformation are presented in the table in Fig. 2. As an illustration consider the case of unit curvature. If a homogeneous beam is subjected to pure bending with a curvature equal to unity, then the difference in u-displacements between two points separated by the unit cell distance (L) will be equal to Lz, and the difference in w-displacements between those points will be equal to $-L^2/2$. This can be verified from the elementary beam formulas.

3.3 Forces on the unit cell

In this section various relationships between the nodal forces that will result from the unit-cell analysis are discussed. Referring to Fig. 2, the corner nodes have numbers 1 to 4. Node i is a typical node on side 1–4 and node j is the corresponding node on side 2–3. Since tractions on the opposite faces of the unit cell are equal and opposite, the following relationships between the nodal forces are obtained:

$$F_{xi} = -F_{xj} \tag{12}$$

$$F_{zi} = -F_{zj} \tag{13}$$

$$F_{z1} = -F_{z2} \tag{14}$$

Now the equilibrium in z direction requires that

$$F_{z3} = -F_{z4} \tag{15}$$

From the condition for equilibrium in the x direction the following is obtained:

$$F_{x1} + F_{x2} + F_{x3} + F_{x4} = 0 \tag{16}$$

Taking moments of all forces acting on the unit cell about node 1, gives

$$(F_{x3} + F_{x4})h = VL \tag{17}$$

where V is the shear force acting on the unit cell. The bending moment at $x=0$ is given by

$$M(0) = \left(\frac{h}{2}\right)F_{x1} - \left(\frac{h}{2}\right)F_{x4} - \sum_i z_i F_{xi} \tag{18}$$

the bending moment at $x=L$ is given by

$$M(L) = \left(\frac{h}{2}\right)F_{x3} - \left(\frac{h}{2}\right)F_{x2} + \sum_j z_j F_{xj} \tag{19}$$

Since the bending moment has a linear variation along x, the bending moment at the center of the unit cell, M_c, is the average of $M(0)$ and $M(L)$. Using eqns (18) and (19) an expression for M_c can be obtained as

$$M_c = \left(\frac{h}{2}\right)(F_{x1} + F_{x3}) + \sum_j z_j F_{xj} \tag{20}$$

It may be noted that $M(0)$ and $M(L)$ are in general not equal, thus violating the applicability of unit-cell approach. From eqns (17)–(19) the jump in bending moment $\bar{M}$—difference between $M(L)$ and $M(0)$—can be computed as

$$\bar{M} = VL \tag{21}$$

Now it is clear that the jump is caused only by the presence of the shear force V, and is indicative of the fact that the steady-state loading condition is not satisfied. In fact this is the magnitude of the periodic couple shown in Fig. 1(c). The couple manifests itself as a pair of equal and opposite forces at the corner nodes 2 and 3, and also 1 and 4. As will be seen later, when $V \neq 0$, these four concentrated forces causes severe distortion at the corners of the unit cell. If $V=0$, then $M(0)=M(L)$, and since the bending moment variation is linear, M will be constant along the unit cell.

3.4 Determination of stiffness coefficients

As described above the three linearly independent deformations are applied to the unit cell. For each case, the axial force P, the bending moment at the center of the unit cell M_c and the shear force V are computed from the nodal forces at the ends of the unit cell. Note that M_c can be computed from eqn (20). From the results a pseudo-stiffness matrix $[k]$ can be computed that relates the deformations and the forces as

$$\begin{bmatrix} k_{11} & k_{12} & k_{13} \\ k_{21} & k_{22} & k_{23} \\ k_{31} & k_{32} & k_{33} \end{bmatrix} \begin{Bmatrix} \epsilon_0 \\ \kappa \\ \gamma_0 \end{Bmatrix} = \begin{Bmatrix} P \\ M_c \\ V \end{Bmatrix} \tag{22}$$

For example, k_{11}, k_{21} and k_{31} will correspond to the values of P, M_c and V obtained for the case of unit axial extension of the unit cell (Case I). The stiffness matrix $[k]$ will not be symmetric because it does not relate corresponding forces and deformations (conjugate quantities, product of which yields an energy term), rather it can be considered as a matrix of influence coefficients. The inverse of $[k]$, denoted by $[s]$, has some significance. The $[s]$ is defined as

$$\begin{bmatrix} s_{11} & s_{12} & s_{13} \\ s_{21} & s_{22} & s_{23} \\ s_{31} & s_{32} & s_{33} \end{bmatrix} \begin{Bmatrix} P \\ M_c \\ V \end{Bmatrix} = \begin{Bmatrix} \epsilon_0 \\ \kappa \\ \gamma_0 \end{Bmatrix} \tag{23}$$

If $V=0$, a steady-state loading condition is obtained, and then $M_c = M$. Noting that only the last column of $[s]$ multiplies with V, and comparing eqns (11) and (23) one can conclude that the first two columns of $[S]$ and $[s]$ should be identical to each other. Since $[S]$ is symmetric ($S_{12}=S_{21}$ and $S_{13}=S_{31}$), all but S_{33} are determined from $[s]$. Estimation of shear compliance S_{33} poses some difficulties. However, a procedure is suggested in the next section.

3.5 Estimation of shear stiffness K_{33}

The difficulty in estimating S_{33} (or K_{33}) is associated with the inability to create a state of deformation such that only V is present. The shear modulus G_{xz} of the material can be computed easily by using the procedure explained in section 2. But it will be based on the assumption that the unit cells span the material in the z direction also. There will be tractions present on the top and bottom surfaces of the beam, and in fact this situation corresponds to Fig. 1(d). One may surmise that a shear correction factor κ^2 could be found such that $K_{33} = \kappa^2 G_{xz} h$. But a simple bimaterial beam example will show that the shear stiffness K_{33} can be grossly underestimated.

Consider a bimaterial beam with layers of equal thickness ($h/2$). From the unit-cell analysis explained in section 2 the shear modulus G_{xz} is found to be equal to $2G_1G_2/(G_1+G_2)$. Assuming $G_1/G_2 = 10$, $G_{xz} = 0{\cdot}182G_1$. Whereas the actual shear stiffness $K_{33} = \kappa^2(G_1+G_2)h/2$, which means that the apparent shear modulus $G_{xz} = (G_1+G_2)/2 = 0{\cdot}55G_1$. This is about three times the previous estimate. Actually this discrepancy is due to differing assumptions regarding the constancy of shear stress or shear strain. The unit-cell analysis of section 2 imposes constant shear stresses in the two materials, and hence the compliance of the composite is the average of compliances of the constituents. This is true when there are large number of unit cells in the z direction. In reality, in a bimaterial beam the shear strain is almost constant in the two layers, and the shear stiffness is the average of the shear stiffness of the individual layers, which is consistent with the method of computing A_{55} in the lamination theory. This illustrates the need for special procedures for computing the shear stiffness of thin textile composite beams.

In what follows a method is proposed for estimating the shear stiffness K_{33} (or the shear compliance S_{33}) of thin textile composites. Consider a beam of length $2L$, consisting of two unit cells, modeled by plane finite elements. The beam is subjected to boundary conditions corresponding to pure shear strain (third boundary condition in the table in Fig. 2). The top and bottom surfaces of the beam are free of tractions. The shear strain energy over a length L in the middle of the beam, U_s, is computed from the finite element results as

$$U_s = \sum_i (\tfrac{1}{2})\tau_{xz}^{(i)}\gamma_{xz}^{(i)}A_i \tag{24}$$

where $\tau_{xz}^{(i)}$ and $\gamma_{xz}^{(i)}$ are the shear stress and shear strain at the center of the ith element and A_i is the area of the ith element. The summation is performed over elements located in a length L in the middle of the beam.

Next, the shear strain energy over the same length L is computed by using the beam formula:

$$U_s = (\tfrac{1}{2})V\gamma_0 L = (\tfrac{1}{2})V(S_{13}P + S_{23}M_c + S_{33}V)L \tag{25}$$

In the above equation P, M_c and V can be obtained from the finite element results. The coefficients S_{13} and S_{23} have already been estimated. The shear compliance S_{33} is the only unknown, which can be solved by equating the shear strain energy quantities in eqns (24) and (25).

The choice of two unit cells to perform the above analysis deserves an explanation. When this was tried with one unit cell for the cases of isotropic beam and bimaterial beam, the results were not good. The reason was the presence of concentrated forces at the four corners of the unit cell as explained in section 3.3. When two unit cells are used in the model, still the stress concentrations remain at the corners of the beam, however their effects diminish in the middle portion of the beam. As will be seen in the next section, the two unit cell method gave very good K_{33} for both isotropic and bimaterial beams.

4 RESULTS AND DISCUSSION

The procedures described above were demonstrated using (a) an isotropic beam; (b) a bimaterial beam; and (c) a textile composite beam. The dimensions of the unit cell and the yarn architecture were taken from Yoshino and Ohtsuka.[10] The same unit cell dimensions were used for the isotropic and bimaterial cases. The finite-element model of the unit cells and their deformed shape under various independent loading conditions are shown in Figs 3–5. The length and height of the unit cell in all cases were equal to 3·6 and 1·8 mm, respectively. Eight-node isoparametric plane strain elements were used to model the unit cell. The finite element mesh for the isotropic beam and the textile beam were identical to each other.

The properties of the isotropic beam were as follows: Young's modulus = 10 GPa, Poisson's ratio = 0·3, thickness = 1·8 mm. The properties of the bimaterial beam were as follows: Young's moduli = 10 and 100 GPa, Poisson's ratios = 0·3, thickness of each layer = 0·9 mm.

In the case of the textile composite the matrix material was modeled as an isotropic material with Young's modulus = 3·5 GPa and Poisson's ratio = 0·35. The yarn was modeled as a transversely isotropic material, with 23 plane as the plane of isotropy. The yarn direction is assumed to be parallel to the 1 axis. Note that 2 axis and y axis are parallel to each other. The elastic constants of the yarn were as follows: $E_1 = 159$ GPa, $E_2 = E_3 = 10{\cdot}9$ GPa, $\nu_{12} = \nu_{13} = 0{\cdot}38$, $\nu_{23} = 0{\cdot}38$, $G_{12} = 6{\cdot}4$ GPa.

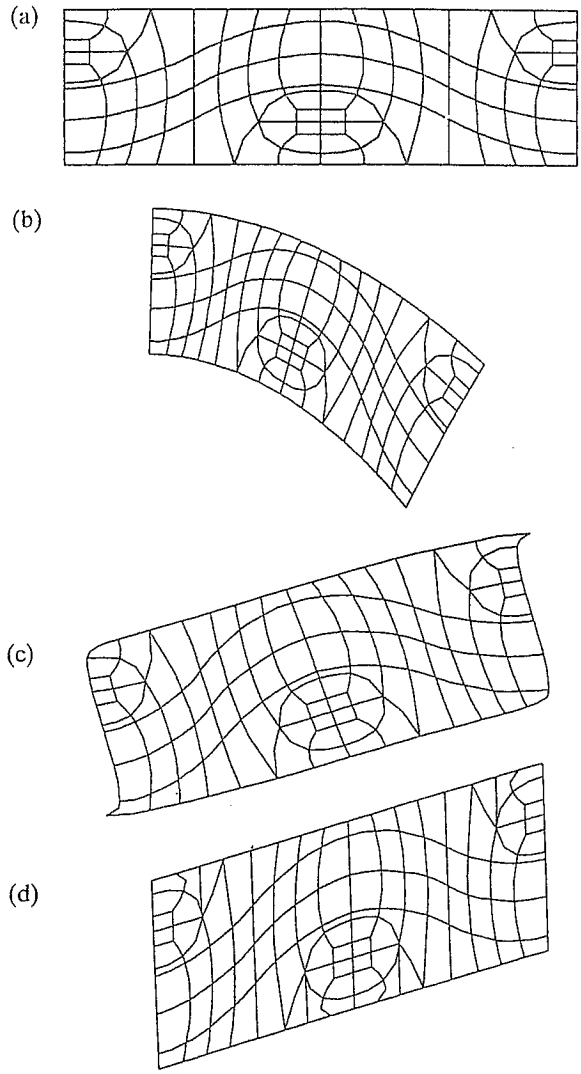

Fig. 3. Deformed unit cell of the isotropic beam subjected to (a) unit extensional strain; (b) unit curvature; (c) unit shear strain, top and bottom surfaces are traction free; and (d) unit shear strain, tractions allowed on top and bottom surfaces (not to scale).

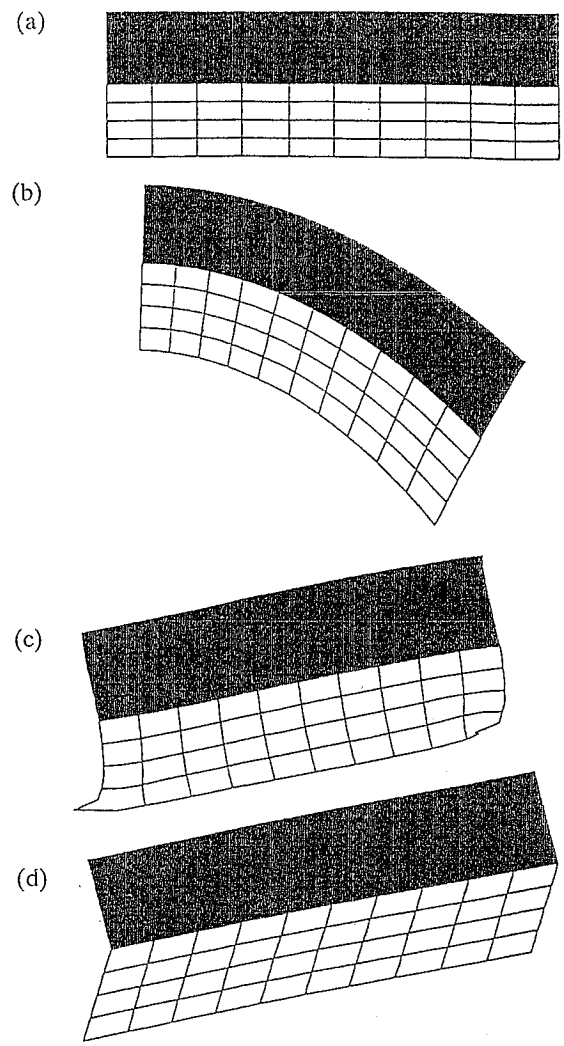

Fig. 4. Deformed unit cell of the bimaterial beam subjected to (a) unit extensional strain; (b) unit curvature; (c) unit shear strain, top and bottom surfaces are traction free; and (d) unit shear strain, tractions allowed on top and bottom surfaces (not to scale).

The results for all cases are presented in Table 1. The results for isotropic and bimaterial beams are compared with exact beam theory solutions. The shear correction factors used for computing A_{55} are 0·833 and 0·555 for the isotropic and bimaterial beams, respectively (Whitney[12]). It may be seen from Table 1 that the present unit-cell analysis is able to predict the stiffness coefficients of isotropic and bimaterial beams. The axial and bending stiffness coefficients are predicted accurately. As expected the shear stiffness predictions have errors, but they are very minimal. One may note the severity of deformation at the corners of the unit cell when subjected to a constant shear strain leaving the top and bottom surfaces traction-free (Figs 3(c), 4(c) and 5(d)). However, when shear tractions are allowed on the top and bottom surfaces of the unit cell, the distortions at the corners disappear (Figs 3(d), 4(d) and 5(e)). Then, what is obtained is actually the shear modulus G_{xz} and not the beam shear stiffness A_{55}. The shear modulus of the textile beam is found to be 3·023 GPa. This will yield $A_{55} = G_{xz}h = 5{\cdot}44 \times 10^6\,\mathrm{N\,m^{-1}}$, whereas the actual A_{55} is $9{\cdot}21 \times 10^6\,\mathrm{N\,m^{-1}}$ (see K_{33} in Table 1). From K_{11} of the textile beam one may extract the Young's modulus E_x as K_{11}/h, which will yield $E_x = 15{\cdot}42$ GPa. If this value is used to determine the flexural stiffness as $D_{11} = E_x h^3/12$, one will obtain $D_{11} = 7{\cdot}50N - m$, whereas the actual flexural stiffness is equal to $5{\cdot}41N - m$ (K_{22} in Table 1). This further illustrates the importance of the present analysis in predicting beam stiffness properties directly.

The stiffness properties of the textile composite were also estimated using a procedure similar to the mosaic model.[1] They are compared with results

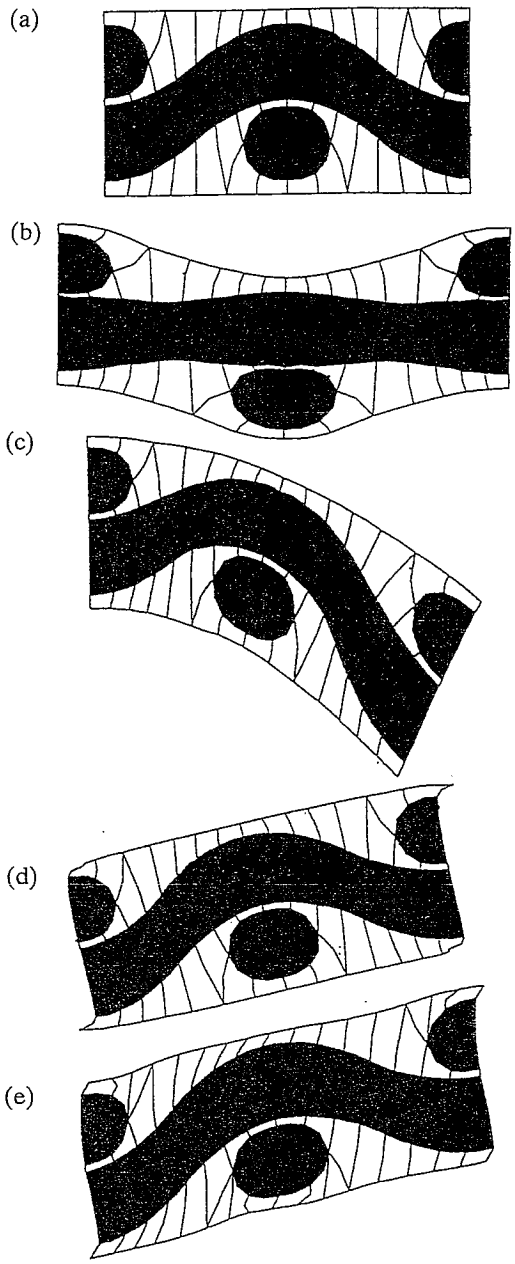

Fig. 5. Textile beam: (a) undeformed unit cell, and deformation under (b) unit extensional strain; (c) unit curvature; (d) unit shear strain, top and bottom surfaces are traction free; and (e) unit shear strain, tractions allowed on top and bottom surfaces (not to scale).

obtained from the present unit cell analysis in Table 1. Figure 6 depicts the idealization made in the mosaic model. The unit cell is divided into five segments, each one idealized as laminates consisting of 0° and 90° layers with different stacking sequences. Reference 1 describes procedures for computing A_{11}, B_{11} and D_{11} (K_{11}, K_{12} and K_{22} in this paper's notation) of woven composites using the mosaic model. The mosaic model can be extended to compute $A_{55}(K_{33})$ also. The stiffness matrix of each segment of the unit cell is computed using the laminate analysis. Then the compliance of the composite is the length-weighted average of compliances of the five segments:

$$[S] = \left(\frac{1}{L}\right) \sum_i L^{(i)}[S]^{(i)} \tag{26}$$

where L_i is the length of the ith segment, and L is the length of the unit cell.

From Table 1 it can be seen that the mosaic model predicts $K_{33}(A_{55})$ reasonably well. The reason for lack of agreement in $K_{11}(A_{11})$ and $K_{22}(D_{11})$ can be attributed to the fact that the fiber undulations are not accounted properly, and a major portion of the yarn is modeled as 0° laminate in the mosaic model, which tends to over predict the in-plane axial and flexural stiffness properties.

The coupling coefficients K_{13} and K_{23} were identically equal to zero for all three beams in all the methods used in this study. It is not a surprising result for isotropic and bimaterial beams. In the case of textile beam, the yarns are symmetrical about a vertical line passing through the center of the unit cell, and that removes the coupling between in-plane forces and transverse shear deformation. Further the extension/bending coupling B_{11} (represented by K_{12})

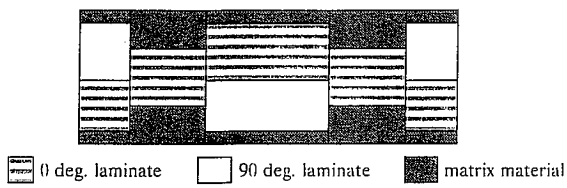

Fig. 6. A mosaic model of the unit cell (not to scale).

Table 1. Comparison of beam stiffness coefficients (SI units)[a]

	Isotropic beam		Bimaterial beam		Textile beam	
	Unit cell analysis	Exact	Unit cell analysis	Exact	Unit cell analysis	Mosaic model
K_{11}	$19{\cdot}78 \times 10^6$	$19{\cdot}78 \times 10^6$	10.88×10^7	$10{\cdot}88 \times 10^7$	$27{\cdot}76 \times 10^6$	$71{\cdot}48 \times 10^{-6}$
K_{12}	0	0	40.05×10^3	$40{\cdot}05 \times 10^3$	0	0
K_{22}	5·35	5·34	29.37	29·37	5·41	8·13
K_{33}	$5{\cdot}96 \times 10^6$	$5{\cdot}77 \times 10^6$	20.82×10^6	$21{\cdot}12 \times 10^6$	$9{\cdot}21 \times 10^6$	$8{\cdot}14 \times 10^6$

[a] The coupling coefficients K_{13} and K_{23} are equal to zero in all cases.

also did not exist for the textile beam. This is again because of the symmetry about the center. The bending/extension coupling that exists in the left half of the unit cell will be nullified by an opposite coupling effect exhibited by the right half of the unit cell. One should note that these are effects averaged over the length of the unit cell. In fact Fig. 5(b) illustrates the existence of bending/extension coupling in the middle portion of the textile composite unit cell.

There are several interesting features in the deformed shapes of the unit cells presented in Figs 3–5. Figures 3(a), 3(b) and 3(d) for the isotropic beam represent pure extension, pure bending and pure shear, respectively. In Fig. 3(c) concentrated forces act at the corners of the unit cell and they cause localized distortion. One may note that the left edge of the deformed unit cell fits the right edge as pieces of puzzle fit together. This is because of the periodic displacement boundary conditions applied to the unit cell. In the case of a bimaterial beam, plane sections remain plane for pure extension and pure bending (Figs 4(a) and 4(b)). There is a marked difference between Figs 4(c) and 4(d). In Fig. 4(c), the beam is more or less in a state of constant shear strain, which is typical of composite beams. In Fig. 4(d) the bottom layer shears significantly, and the top layer undergoes minimal shear deformation. This is because of the fact the application of shear tractions on the top and bottom surfaces of the unit cell, causes a constant shear state within the unit cell. The bottom layer being very compliant ($G_{top}/G_{bottom} = 10$) undergoes severe shear strain compared to the top layer. As mentioned earlier the existence of localized bending/extension coupling in the textile beam can be observed in Fig. 5(b).

5 SUMMARY

The unit cell of a textile composite beam was analyzed to determine the flexural stiffness properties. The unit cell was modeled using eight-node plane strain finite elements. Three linearly independent deformations were applied to the unit cell. Special constraint elements were used to apply periodic boundary conditions on the end faces of the unit cell. From the forces required to create such deformations, the extensional, flexural and shear stiffness of the beam were computed. The method was verified by applying to isotropic and bimaterial beams, and comparing the results with the beam theory and the lamination theory. The agreement was excellent. Then the method was used to obtain the stiffness coefficients of a plain weave composite modeled as a beam. The transverse shear stiffness was determined by a modified method in which the shear strain energy of the unit cell in the finite element model was equated to the shear strain energy in the beam model. The beam example presented here should be considered as a demonstration of the unit cell approach to predict the flexural stiffness properties similar to Refs 5 and 10. In practice, one needs to find the complete $[A, B, D]$ matrices including the transverse shear stiffness coefficients A_{44}, A_{45} and A_{55}. The present technique has been extended to compute the $[A]$, $[B]$ and $[D]$ matrices of textile composite plates by using three-dimensional solid elements to model the unit cell.[13] Extension of the present method to predict thermal conductivities and coefficients of thermal expansion is also straightforward and is under way.

ACKNOWLEDGEMENT

This research was supported by the NASA Langley Research Center Grant NAG-1-1226 to the University of Florida and the Space Assistantship Enhancement Program (1991) of the Florida Space Grant Consortium.

REFERENCES

1. Ishikawa, T. & Chou, T. W., Stiffness and strength behavior of woven fabric composites. *J. Mater. Sci.*, **17** (1982) 3211–20.
2. Ishikawa, T. & Chou, T. W., Elastic behavior of woven hybrid composities. *J. Comp. Mater.*, **16** (1982) 2–19.
3. Ishikawa, T. & Chou, T. W., In-plane thermal expansion and thermal bending coefficients of fabric composites. *J. Comp. Mater.*, **17** (1983) 92–104.
4. Ishikawa, T. & Chou, T. W., Thermoelastic analysis of hybrid fabric composites. *J. Mater. Sci.*, **18** (1983) 2260–8.
5. Ishikawa, T. & Chou, T. W., One dimensional micromechanical analysis of woven fabric composites.. *AIAA J.*, **21** (1983) 1714–21.
6. Yang, J. M. & Chou, T. W., Performance maps of textile structural composites. In *Sixth International Conference on Composite Materials (ICCM VI)*. 1987, **5**:5.579–5.588.
7. Ma, C. L., Yang, J. M. & Chou, T. W., Elastic stiffness of three-dimensional textile structural composites. In *Composite Materials: Testing and Design (Seventh Conference)* (ASTM STP 893). 1986 pp. 404–21.
8. Foye, R. L., Approximating the shear field within the unit cell of a fabric reinforced composite using replacement elements, NASA CR-189597, February 1993.
9. Whitcomb, J. D., Three-dimensional stress analysis of plane weave composites. In *Composite Materials Fatigue and Fracture (Third Volume)* (ASTM STP 1110). 1991, pp. 417–38.
10. Yoshino, T. & Ohtsuka, T., Inner stress analysis of plane woven fiber reinforced plastic laminates. *Bull. JSME*, **25–202** (1982) 485–92.
11. Dasgupta, A. & Bhandarkar, S., Pecht, M. & Barker, D., Thermoelastic properties of woven-fabric composites using homogenization techniques. In *Proceedings of the American Society for Composites. Fifth Technical Conference.* Technomic Publishing Co. Inc., Lancaster, PA, USA, 1990, pp. 1001–10.

12. Whitney, J. M., Shear correction factors for orthotropic laminates under static load. *J. Appl. Mech.*, **40** (1973) 302–4.
13. Sankar, B. V. & Marrey, R. V., A unit cell analysis for predicting the [A], [B], [D] matrices of a textile composite plate. Technical Note CAC-TN-92-01, Center for Advanced Composites, University of Florida, Gainesville, FL, USA.